

# Time reversibility of Lamb waves in thin plates with surface-bonded piezoelectric transducers is temperature invariant at the best reconstruction frequency

Structural Health Monitoring

1–15

© The Author(s) 2020

Article reuse guidelines:

[sagepub.com/journals-permissions](https://sagepub.com/journals-permissions)

DOI: 10.1177/1475921720965122

[journals.sagepub.com/home/shm](https://journals.sagepub.com/home/shm)

Bhabagrahi Natha Sharma<sup>1</sup> , Santosh Kapuria<sup>2,3</sup>  and A Arockiarajan<sup>1</sup>

## Abstract

The Lamb wave time-reversal method has been widely proposed as a baseline-free method for damage detection in thin-walled structures. Under varying thermal environments, it would require that the time reversibility of Lamb waves is temperature invariant. In this study, we examine the temperature dependence of Lamb waves and its time reversibility using experiments and finite element simulations on isotropic plates with surface-bonded piezoelectric wafer transducers for actuation and sensing. The study is conducted at three different temperatures of the system from 25°C to 75°C for a wide range of excitation frequency. The results indicate that the time reversibility can undergo significant changes due to temperature variations depending on the excitation frequency. However, at the best reconstruction frequency corresponding to the maximum similarity of the reconstructed signal with the original input signal (proposed recently as the probing frequency), the change in the percent similarity with temperature is insignificant. The results also demonstrate that changes in the physical properties of both adhesive layers and piezoelectric transducers with temperature play a dominant role in influencing Lamb wave amplitudes. However, only the change in the characteristics of the adhesive layers is responsible for the temperature dependence of the time reversibility of Lamb waves.

## Keywords

Time-reversal method, Lamb wave, temperature variation, time reversibility, best reconstruction frequency, structural health monitoring

## Introduction

Lamb wave-based techniques are gaining immense popularity for structural health monitoring (SHM) applications to detect internal and surface damages in thin-walled structures, such as aerospace structures, pressure vessels, pipelines and so on, using embedded and surface-bonded transducers.<sup>1</sup> Lamb waves possess the advantage of the ease of generation, ability to travel a long distance with minimal amplitude attenuation and covering a large area with less number of sensors. The damage detection using Lamb waves conventionally relies on a comparison of the damage features, such as the amplitude and the time of flight, with the baseline response previously obtained from the same structure in its pristine condition. The interaction of the propagating Lamb waves with the damage causes their

scattering, resulting in a change in the time of flight and the amplitude of the response signal. However, such changes can also be caused by a change in the operating temperature of the structure, leading to possible false alarms for damage<sup>2</sup> unless suitable compensation is made to the signals.

<sup>1</sup>Department of Applied Mechanics, Indian Institute of Technology Madras, Chennai, India

<sup>2</sup>CSIR-Structural Engineering Research Centre, Chennai, India

<sup>3</sup>Department of Applied Mechanics, Indian Institute of Technology Delhi, New Delhi, India

## Corresponding author:

Santosh Kapuria, Department of Applied Mechanics, Indian Institute of Technology Delhi, New Delhi 110016, India.

Email: [kapuria@am.iitd.ac.in](mailto:kapuria@am.iitd.ac.in)

To identify the influence of temperature on Lamb wave propagation, an experimental study was performed by Blaise and Chang<sup>3</sup> on a sandwich panel with embedded piezoelectric transducers in pitch-catch configuration at cryogenic temperature ( $-90^{\circ}\text{C}$ ). The experiments revealed that the amplitude and the time of arrival of the response signal decreased with a decrease in the temperature. Another experimental study was conducted by Lee et al.<sup>4</sup> for temperature ranging from  $35^{\circ}\text{C}$  to  $70^{\circ}\text{C}$ , by symmetrically arranging two piezoceramic actuators on an aluminium plate and exciting only the symmetric fundamental mode  $S_0$ . A comparison was made between the influences of temperature and presence of damage on the Lamb wave response by conducting the experiments on the plate in the healthy condition and with a hole of 1 mm diameter placed at the centre. The study revealed that both the increase in temperature and the presence of damage cause a decrease in the amplitude of the response signal and an increase in its time of arrival. However, the effect of temperature was so significant that it dwarfed the signal changes observed when the damage was introduced. Chambers et al.<sup>5</sup> reported a drop in the amplitude of the pulse-echo response of a piezoelectric transducer bonded on an aluminium beam, clamped with steel boundary clamps, with the increase in temperature to  $85^{\circ}\text{C}$ . They attributed this drop to the degradation of the shear couplant between the beam and the boundary clamps, reducing the reflections. The effect of temperature rise (up to  $240^{\circ}\text{C}$ ) on the sensor response of the piezoelectric patch transducer used for free vibration analysis of an aluminium beam was investigated by Schulz et al.<sup>6</sup> The sensor signal amplitude decreased with increasing temperature, eventually reducing to the noise level at  $240^{\circ}\text{C}$  because of the depoling of the piezoelectric transducer. The effect of temperature on the fundamental antisymmetric Lamb wave mode  $A_0$  was investigated experimentally by Konstantinidis et al.<sup>7</sup> for a rather small temperature range of  $22^{\circ}\text{C}$ – $32^{\circ}\text{C}$  in an aluminium plate. In this case too, the time of arrival of the response signal was affected, which was attributed to the thermal expansion/contraction and change in the material density, thickness and the elastic modulus of the plate. In addition, the central frequency of the response signal showed a shift with temperature, which was credited to the change in the transducer frequency response caused by the change in the piezoelectric properties of the transducer and the change in the adhesive stiffness.

While the aforementioned studies were conducted on Lamb waves generated by narrowband excitations, such as the Hann window-modulated tone burst signals, Lu and Michales<sup>8</sup> studied the effect of temperature on diffuse ultrasonic waves generated by broadband impulse

excitations and formed after multiple reflections. The results (obtained for a temperature range of  $5^{\circ}\text{C}$ – $40^{\circ}\text{C}$ ) revealed that for the diffuse waves too, the time of arrival of the waveform increased with the increase in temperature, owing to the thermal expansion and the change in the material properties of the plate.

In addition to the experimental studies on the effect of temperature on the Lamb wave propagation, researchers have also employed different numerical and analytical models for the Lamb wave propagation to understand the relative contributions of the changes in the mechanical and electrical properties of the constituent elements (plate, piezoelectric transducer and adhesive layer) with the change in temperature. Raghavan and Cesnik<sup>9</sup> employed a three-dimensional (3D) elasticity-based analytical solution to study the pitch-catch response of the PZT-5A patch transducers bonded to an aluminium plate over a temperature range from  $20^{\circ}\text{C}$  to  $150^{\circ}\text{C}$ . They compared the analytical predictions with experimental results. The analytical solution predicted the delay in the time of arrival of the  $S_0$  mode waveform with increasing temperature, as observed in the experiments. The results revealed that the peak amplitude of the sensor response increased with the rise in temperature up to  $90^{\circ}\text{C}$ , beyond which it showed a decrease up to a temperature of  $150^{\circ}\text{C}$ . It was shown that Young's moduli of the PZT-5A transducers and the aluminium plate, and the piezoelectric constants of PZT-5A are thermally sensitive, which influences the sensor signal. This study also revealed that the temperature change may not affect the detection of a mild damage (e.g. indentation of half thickness) up to a certain temperature. However, at higher temperatures, the change in the response due to the temperature variation may become comparable to that caused by the damage, leading to a reduced detection sensitivity. Subsequently, Scalia and Salamone<sup>10</sup> used PZT-5A and microfiber composite pairs as transducers bonded on an aluminium plate in the pitch-catch configuration to study the effect of temperature on the Lamb wave response, experimentally and using a plane strain-based two-dimensional (2D) analytical solution, for the temperature range from  $-40^{\circ}\text{C}$  to  $60^{\circ}\text{C}$ . Like in the study of Raghavan and Cesnik,<sup>9</sup> here too, the results showed an increase in the amplitude of the sensor signal with an increase in temperature from  $-40^{\circ}\text{C}$  to  $20^{\circ}\text{C}$ , followed by a decrease up to  $60^{\circ}\text{C}$ . The competing roles of the piezoelectric coefficients and the dielectric permittivities of the transducers were shown to be responsible for this trend in the variation of the sensor response. Some studies<sup>11,12</sup> using experimental measurements, analytical predictions and finite element (FE) simulations reported that a temperature change over a large range from  $-18^{\circ}\text{C}$  to  $107^{\circ}\text{C}$  caused only

small changes in the wave propagation response in a plate structure, mainly as a change in the time of arrival. They, however, neglected the temperature effects on the piezoelectric transducers and adhesive layers and considered only the normalized sensor response. The role of the adhesive layer on the Lamb wave propagation in structures at elevated temperatures was investigated by Ha et al.<sup>13</sup> using 3D numerical simulations as well as experiments for a temperature range of 25°C–75°C. It was concluded that among all the material constants involved, the stiffness change of the adhesive layer due to the temperature variation has the maximum influence on the sensor signals. In a recent study, Kijanka et al.<sup>14</sup> employed the 3D FE solutions, validated with experimental measurements, to delineate the influences of temperature-induced changes in the physical properties of the individual elements, that is, the PZT, adhesive layer and the host structure, on the Lamb wave response.

To address the issue of the temperature dependence of the baseline signals of healthy structures, several temperature compensation strategies, such as optimal baseline selection,<sup>8</sup> baseline signal stretch<sup>15</sup> and the cointegration technique,<sup>16</sup> have been proposed for damage detection in a variable temperature environment. However, the collection of baseline data at various temperatures for all possible operating conditions for an existing structure, may not always be possible or if possible, is likely to demand enormous storage space posing another challenge. To overcome this problem, baseline-free damage detection methods are being pursued in the recent past. Among various techniques, the one based on the time-reversal process (TRP) of Lamb waves has emerged as the most promising candidate for damage detection in thin-walled structures.

Initially used in acoustic by Fink,<sup>17</sup> the TRP is based on the principle of reciprocity and the time-reversal invariance of the linear acoustic wave equation. In this process, the original input signal can be reconstructed back at the source transducer by emitting back the time-reversed version of the forward response signal obtained at the receiver. In a perfectly healthy structure, the reconstructed waveform would exactly match with the original input signal. In contrast, the presence of the damage causes nonlinear changes in the wave propagation response, leading to a mismatch between the reconstructed signal and the input signal. However, unlike in acoustics, time reversibility is not perfect in the case of Lamb waves, even in a healthy structure because of amplitude dispersion, which is not compensated during the TRP.

Several studies have employed the time-reversal method (TRM) for damage detection in metallic and laminated composite plates using single-mode ( $S_0$  or  $A_0$ )<sup>18,19</sup> and multiple-mode<sup>20,21</sup> actuation of Lamb waves. These studies, however, reported conflicting trends on the sensitivity of the reconstructed signal to the presence of damage, raising a concern on efficacy of the TRM for damage detection. To comprehend these conflicting results, Agrahari and Kapuria<sup>22,23</sup> investigated the TRM in an aluminium plate with surface-bonded piezoelectric transducers using experiments as well as FE simulations. Their study unveiled for the first time the inability of single-mode tuning of Lamb waves at the so-called sweet spot frequency, recommended by many researchers, to attain the best time reversibility in healthy plate structures. They proposed to perform the TRP at an excitation frequency called the best reconstruction frequency at which the similarity between the reconstructed signal and the original input is the maximum over a desired range of excitation frequency. A refined time-reversal method (RTRM) was also introduced with damage indices computed using extended modes of the reconstructed signal, which yielded excellent sensitivity to the presence of damage.

The success of the TRP as a true baseline-free method in the presence of expected environmental variability during operation of a structure, however, stands on the presumption that the time reversibility of the Lamb wave is invariant of the temperature and other environmental variations. A time-reversal-based self-diagnostic scheme for piezoelectric transducers has been developed explicitly considering temperature effects to distinguish debonding in the transducer from the crack using temperature variations.<sup>24</sup> In this case, the TRM was modified to be employed in a single transducer configuration between the electrical potential as input and mechanical response of the transducer as output. The results showed that the time reversibility was affected by temperature variation within the studied range of  $-5^{\circ}\text{C}$ – $53^{\circ}\text{C}$ . However, no study has been reported so far on how temperature variation influences the time reversibility of Lamb waves in a pitch-catch configuration for damage detection. Such a study is essential to ascertain the applicability of the TRM as a baseline-free method of damage detection in the presence of varying operating temperature.

In this article, we present a detailed investigation on the effect of temperature on the forward response and time reversibility of Lamb waves in thin metallic plates, actuated and sensed by surface-bonded piezoelectric

wafer transducers. The study employs both experiments and numerical simulations. The aim is to ascertain whether or not the TRM and/or the newly developed RTRM can be successfully used for baseline-free damage detection in the presence of temperature variations.

## Time reversibility

Damage detection using the TRP is conducted by comparing the reconstructed signal with the original input signal, after normalizing both the signals with their corresponding peak amplitudes. The presence of damage affects the time reversibility of the forward wave response due to its nonlinear interaction with the damage, and consequently, the reconstructed waveform shows deviation from the input waveform. The quality of time reversibility is quantified by percent similarity based on the  $L_2$  error norm as<sup>25</sup>

$$\%Similarity = \left( 1 - \sqrt{\int_{t_i}^{t_f} [V(t) - I(t)]^2 dt / \int_{t_i}^{t_f} I^2(t) dt} \right) \times 100 \quad (1)$$

where  $V(t)$  and  $I(t)$  denote the normalized reconstructed and original input signals, respectively, and  $t_i$  and  $t_f$  denote, respectively, the start and end time instances of the signals under comparison.

Conventionally, the main mode waveform of the reconstructed signal obtained through the TRP is considered for comparison with the input signal waveform. However, it has been shown earlier that the presence of damage may cause only a marginal distortion in the main mode waveform of the reconstructed signal, whereas it creates extra bands between the main mode and the two side bands of the reconstructed signal.<sup>22</sup> Since the extra bands offer distinct features indicating the presence of damage, Agrahari and Kapuria<sup>22</sup> proposed to include them for comparison with the input signal using an extended mode signal ranging between the two side bands of the reconstructed signal (Figure 1). It resulted in excellent sensitivity of the damage indices to the presence of damage. The same method is followed in this study. The start and end time instances of the reconstructed signal inclusive of the extra modes are specified as

$$t_i = t_m - t_s + t_{sl}/2, \quad t_f = t_m + t_s - t_{sl}/2$$

where  $t_m$  is the time instance of the peak of the main wave packet of the reconstructed signal,  $t_s$  denotes the time interval between the peaks of the main waveform and the side band and  $t_{sl}$  is the time span of the main mode wave packet.  $t_s$  can be determined from experimental data or estimated theoretically as  $t_s = d/V_{A_0} - d/V_{S_0}$ , where  $d$  is the centre-to-centre distance between

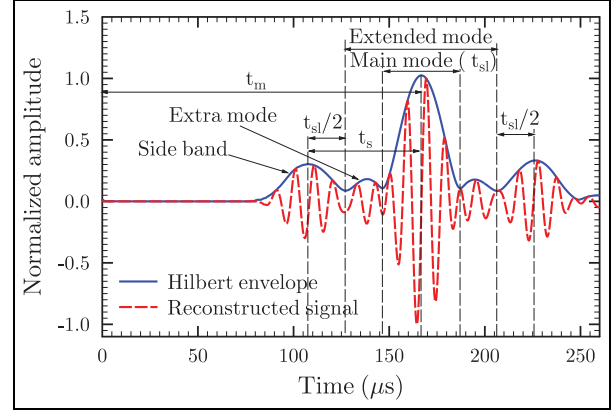


**Figure 1.** Reconstructed signal along with Hilbert envelope showing main mode and extended mode for a damaged plate.

the transducers, and  $V_{S_0}$  and  $V_{A_0}$  denote the group velocities of the  $S_0$  and  $A_0$  modes, respectively.

## Experimental setup

We used an aluminium plate of size 1500 mm  $\times$  1200 mm  $\times$  3 mm as the host structure for the experiments (Figure 2). The actuator and sensor used for the Lamb wave actuation and sensing were two square-shaped piezoelectric transducers (SP-5H) of size 10 mm and thickness 0.25 mm made by Sparkler Ceramics, India. They were bonded to the top surface of the plate using the commercially available two-part Araldite epoxy adhesive, in the pitch-catch configuration with a centre-to-centre distance of 300 mm. The adhesive was cured at room temperature ( $\sim 25^\circ\text{C}$ ) for 48 h before starting the first measurements.

A data acquisition system (QDAM772E18) with sampling rate of 80 mega samples per second (MSPS) and resolution of 14 bit, made by Quazar Technologies Pvt. Ltd, India, was used to generate, amplify, actuate and sense the voltage signal.<sup>26</sup> The data acquisition and signal processing were performed using the iQ: data acquisition and visualization software, developed by the same company. Figure 3 shows schematically the arrangement of the experimental setup.

During the experiment, one of the transducers was actuated with a five-cycle (unless stated otherwise) Hann window-modulated sinusoidal tone burst of 20 V peak amplitude. The Hann window-modulated sinusoidal tone burst signal is defined as  $V(t) = (V_0/2) [1 - \cos(2\pi t/T_H)] \sin(2\pi f t)$ , where  $f$  denotes the central frequency of the excitation and  $T_H$  represents the Hann window length obtained using the number of cycles in the tone burst  $N_B$  as  $T_B = N_B/f$ . A typical input signal is shown in Figure 4 for a central frequency of 200 kHz.

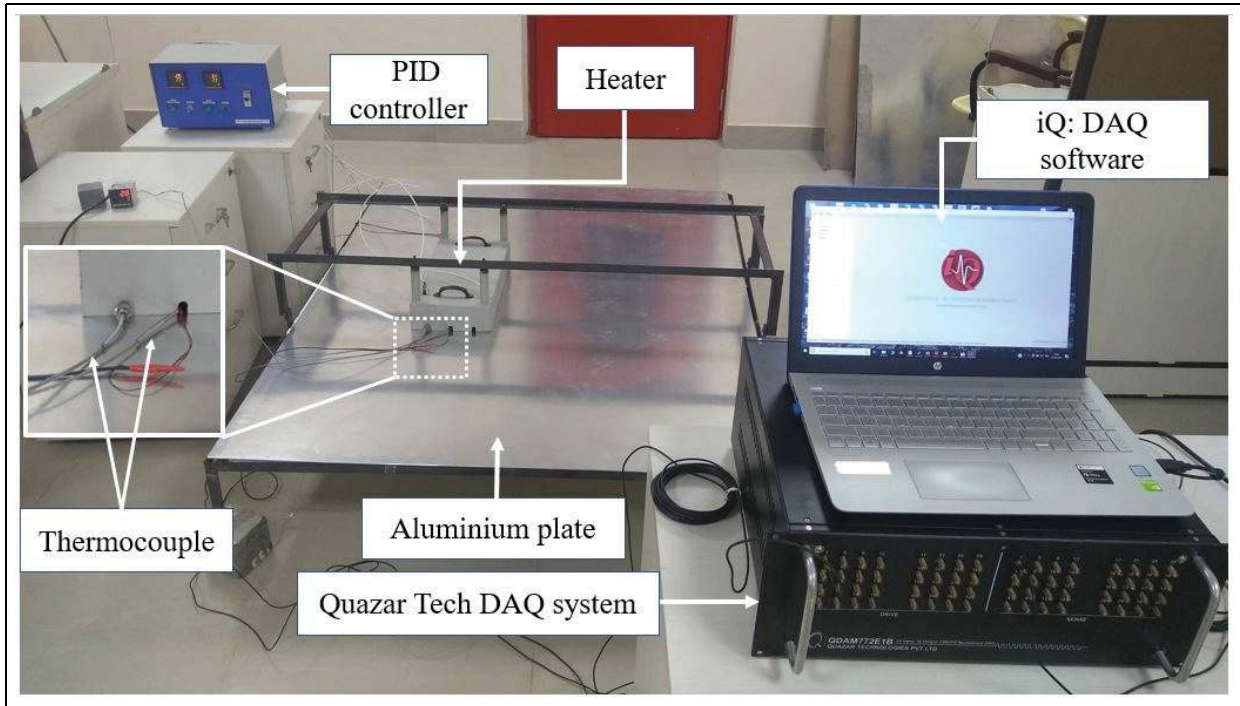


**Figure 2.** Various components of the experimental setup.

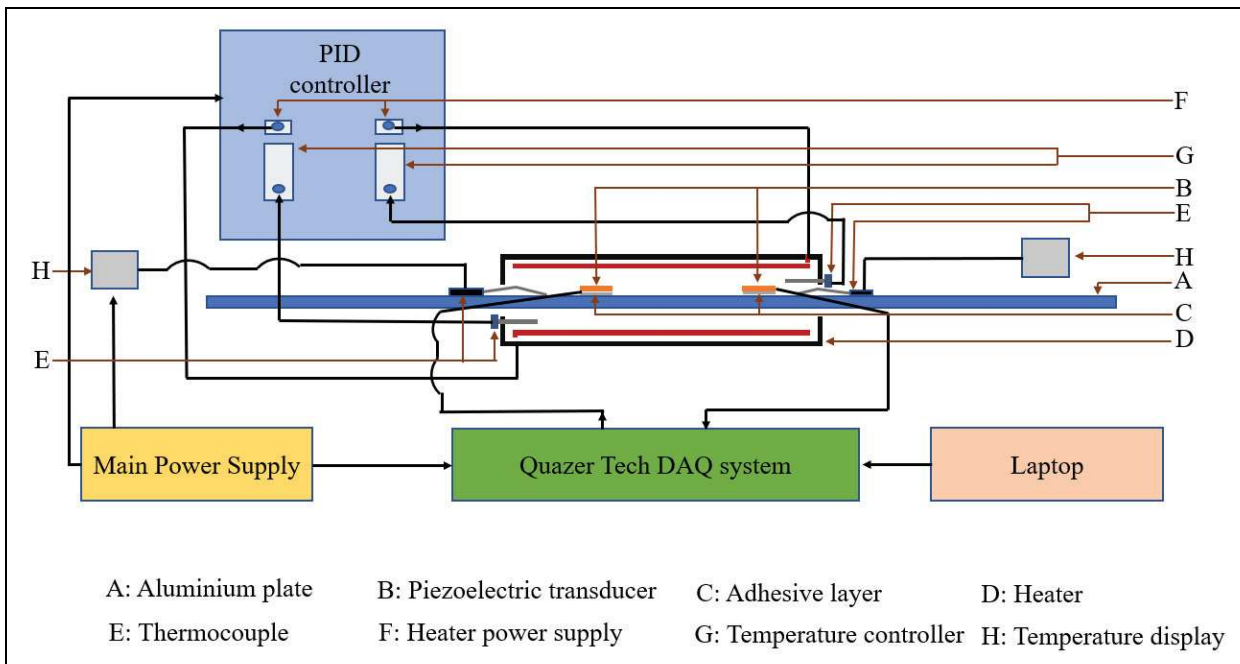


**Figure 3.** Schematic diagram of the experimental setup.

The response signal was recorded at the other transducer after applying a gain of 10 dB. The signals were recorded with a sampling frequency of 72 MSPS. Each measurement was repeated 20 times, and the response

signals were averaged to improve the signal-to-noise ratio. The response signal recorded at the sensor location (forward response) was time-reversed, amplified to the peak amplitude of 20 V and then emitted back to

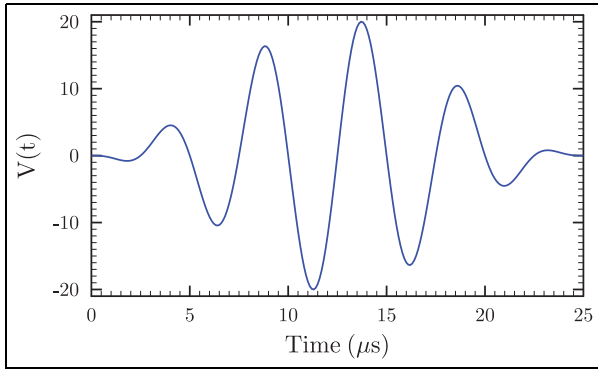


**Figure 4.** Hann window-modulated five-cycle sinusoidal tone burst signal of 200 kHz central frequency.

the source transducer. Then the reconstructed signal was recorded at the source location and compared with the original input signal after normalizing both the signals with their corresponding peaks to evaluate the percent similarity.

The experiments were conducted at different temperatures by heating the plate from both the top and bottom sides using a two-part heater manufactured by Elmec Heaters and Controllers, India. Each part of the heater has a heating area of 400 mm  $\times$  200 mm. The heaters were positioned in a manner to avoid any physical contact with the plate. Two PID controllers with K-type thermocouples were used for the controlled heating of the plate. Two additional K-type thermocouples were placed in the heating area of the plate to monitor the uniformity of the temperature. The experiments were conducted at 25°C, 50°C and 75°C.

## FE model

The FE analysis of the plate adhesive transducer system was performed to validate the experimental observations and also to conduct parametric studies subsequently. The commercially available FE software

ABAQUS Standard is used to perform the analysis. An aluminium plate of length 1500 mm and thickness 3 mm is considered for the FE model. A reduced size of 9 mm was considered for the piezoelectric patches (as against their original size of 10 mm) to account for the expected weak bonding of the adhesive around the edges in the experimental setup. The thickness of the adhesive layer between the transducer and the host plate in the experimental setup was measured using a MICRO-OPTRONIC made laser displacement sensor ILD-1400-20, having a resolution of 2  $\mu$ m, following the procedure discussed in Agrahari and Kapuria.<sup>25</sup> The average thickness of both the adhesive layers was obtained as 50  $\pm$  2  $\mu$ m, which is used in the FE model.

A detailed study on the full-field 3D FE model and a simplified plane strain 2D FE model for the analysis of Lamb wave propagation in such actuator-plate-sensor systems was reported in Agrahari and Kapuria.<sup>25</sup> The study revealed that the 3D FE results match well with the experiments, and although the responses obtained from the 3D and 2D FE models differ in respect of the actual peak amplitude, the normalized responses predicted by them show good agreement. Since the TRP-based method being studied here is concerned with normalized response signals, the plane strain 2D FE model, which requires significantly less computational time than the detailed 3D FE simulation, is employed for the simulation here. Accordingly, the plate and adhesive layers are modelled using the eight-node plane strain quadrilateral element (CPE8R) with reduced integration. The piezoelectric transducers are modelled using the eight-node plane strain piezoelectric quadrilateral element (CPE8E). A mesh size of 0.5 mm  $\times$  0.5 mm is taken for the plate, as shown in Figure 5, which satisfies the requirement of a minimum of 20 elements over the shortest wavelength for good spatial resolution. A finer mesh of length 0.1 mm is used for the transducers, the adhesive layers and the plate in the transducer regions up to 5 mm on both sides of the transducers to accurately model the shear stress transfer at the transducer-

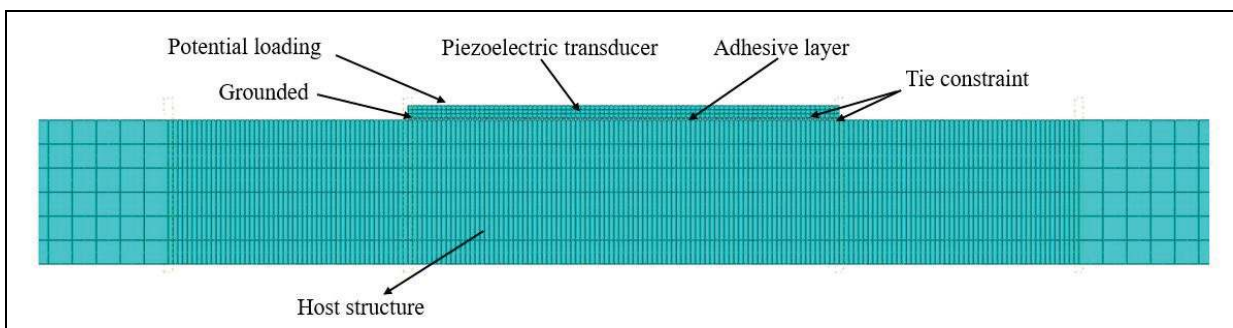


**Figure 5.** Mesh configuration shown for a portion of actuator patch in the 2D FE model.

**Table 1.** Material properties.

Material	$Y_1$	$Y_2$	$Y_3$	$G_{23}$	$G_{13}$	$G_{12}$	$\nu_{23}$	$\nu_{13}$	$\nu_{12}$	$\rho$ (kg/m <sup>3</sup> )
	(GPa)									
Aluminium <sup>22</sup>	70.30	70.30	70.30	26.42	26.42	26.42	0.33	0.33	0.33	2700
Adhesive <sup>28</sup>	4.70	4.70	4.70	1.67	1.67	1.67	0.4	0.4	0.4	1700
SP-5H <sup>29</sup>	66.67	66.67	47.62	23.00	23.00	23.50	0.51	0.51	0.29	7500
	$d_{31}$	$d_{32}$	$d_{33}$	$d_{15}$	$d_{24}$		$\epsilon_{11}/\epsilon_0^a$	$\epsilon_{22}/\epsilon_0$	$\epsilon_{33}/\epsilon_0$	
	$(\times 10^{-12} \text{ mV}^{-1})$									
SP-5H <sup>29</sup>	-265.0	-265.0	550.0	741	741		3100	3100	3400	

<sup>a</sup>Electrical permittivity of free space  $\epsilon_0 = 8.854 \times 10^{-12} \text{ F/m}$ .<sup>31</sup>

plate interfaces. Along the thickness direction, the transducers are discretized into three elements each, and the adhesive layers are discretized with two elements each. A convergence study has been conducted, and it is observed that the present results are independent of the mesh size with finer meshes.

The tie constraints are applied between the transducer-adhesive and adhesive-plate interfaces. At the top nodes of the piezoelectric transducers, an equipotential condition is imposed by coupling their electric potential degrees of freedom. The interfaces between the piezoelectric transducers and the adhesive layers are electrically grounded. A time step of 100 ns is considered for excitations with central frequencies up to 300 kHz, above which a time step of 50 ns is considered. It satisfies the requirement of at least 20 time steps for one wave cycle for good temporal resolution.<sup>27</sup> For the forward response, the top surface of the actuator is subjected to a five-cycle Hann window-modulated sinusoidal tone burst voltage of 20 V, and the electric potential output is obtained at the top surface of the sensor. For the reconstructed signal, the sensor response is time-reversed and applied at the sensor, and the output is obtained at the source transducer as described earlier in the 'Experimental setup' section.

### Temperature-dependent material properties

The temperature-dependent material properties of the aluminium plate, araldite adhesive and SP-5H type piezoelectric transducers are taken from the available literature. The material properties at the room temperature (25°C) are shown in Table 1. Since the temperature range (25°C–75°C) under consideration is small, the variation of the material properties with temperature is assumed to be linear.

For the SP-5H type piezoelectric transducers, a variation rate of 21 MPa °C<sup>-1</sup> and  $-2 \times 10^{-5} \text{ °C}^{-1}$  with respect to temperature is used for Young's modulus and Poisson's ratio, respectively, following Sherrit

et al.<sup>30</sup> The variation rates of piezoelectric coefficients  $d_{31}$  and  $d_{33}$  and relative permittivities with the increase in temperature are taken as -0.95 pm/V °C, 1.85 pm/V °C and 20.2/°C, respectively.<sup>31</sup> For the aluminium plate, the variation rates of Young's modulus and Poisson's ratio with the temperature are  $-40 \text{ MPa °C}^{-1}$  and  $-3.1 \times 10^{-4} \text{ °C}^{-1}$ .<sup>10</sup> The linear rate of variation of the shear modulus of the araldite adhesive with temperature is considered as  $-77.0 \text{ MPa °C}^{-1}$ .<sup>28</sup> The variation of Poisson's ratio of the adhesive layer with temperature is neglected. The coefficients of thermal expansion of the aluminium plate, piezoelectric transducer and the adhesive are taken as  $23.1 \times 10^{-6}$ ,  $3 \times 10^{-6}$  and  $67 \times 10^{-6} \text{ m/m °C}$ , respectively. First, the deformation analysis is performed at the prescribed elevated temperature (50°C or 75°C). The FE model is regenerated on the deformed shape obtained, and the wave propagation analysis is performed on this model. Thus, the FE simulations for the wave propagation are conducted on three models based on the deformed shapes at the three different temperatures, with the corresponding material properties.

### Material damping

The material damping is modelled as Rayleigh damping given by

$$\mathbf{C} = \alpha \mathbf{M} + \beta \mathbf{K} \quad (2)$$

where  $\mathbf{M}$ ,  $\mathbf{K}$  and  $\mathbf{C}$  denote mass, stiffness and damping matrices, respectively, and  $\alpha$  and  $\beta$  are the mass proportionality and stiffness proportionality damping coefficients, respectively. These constants can be determined from the modal damping ratio  $\xi$  as

$$\xi = \frac{\alpha}{2\omega} + \frac{\beta\omega}{2} \quad (3)$$

where  $\omega = 2\pi f$  is the circular frequency,  $f$  being the frequency in Hz. In this analysis, only the stiffness proportionality damping  $\beta$  is considered. For the

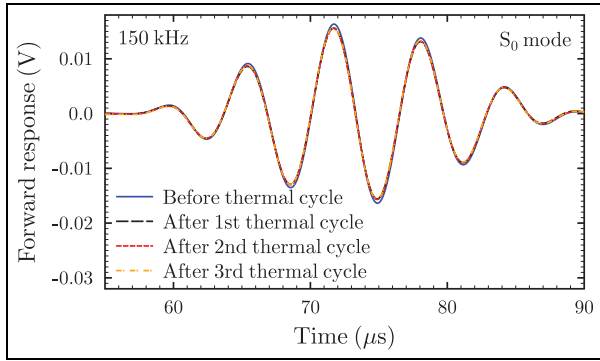


**Figure 6.**  $S_0$  mode of forward Lamb wave response under 150 kHz modulated tone burst excitation measured at room temperature and after each of the three thermal cycles.

considered frequency range, the damping coefficients  $\beta$  for the plate, adhesive layer and the piezoelectric transducer at 25°C are taken as  $5 \times 10^{-10}$ ,<sup>32</sup>  $1 \times 10^{-9}$ ,<sup>33</sup> and  $12.7 \times 10^{-8}$ ,<sup>34</sup> respectively. At the elevated temperatures of 50°C and 75°C, the damping coefficient of the adhesive layer increases to  $23.3 \times 10^{-8}$  and  $31.8 \times 10^{-8}$ , respectively. The change in the the damping constant with temperature rise is neglected for the piezoelectric transducers and the host plate as they are small.

## Results and discussion

### Response of adhesive to repetitive thermal cycles

The experiments began with examining the stability of the Araldite adhesive under repetitive heating and cooling cycles. Before exposing to the first thermal cycle, a forward response signal was recorded by actuating with an input excitation with a central frequency of 150 kHz. Thereafter, the specimen was exposed to repeated thermal cycles by heating to 75°C and

allowing it to cool to room temperature (25°C) by itself. This heating–cooling cycle was repeated thrice. At the end of each thermal cycle, the forward response was recorded. A comparison of the  $S_0$  mode of the forward responses recorded before the first thermal cycle and after every thermal cycle (Figure 6) shows that there is a drop in the amplitude of the response after the application of the first thermal cycle. However, no significant change occurs in the amplitude of the response after the subsequent thermal cycles, which confirms the stability of the Araldite adhesive to repetitive heating cycles. The drop in amplitude after the first thermal cycle can be attributed to the thermal pre-stability of the piezoelectric transducers. Raghavan and Cesnik<sup>9</sup> reported a similar behaviour of piezoelectric transducers under thermal cycles.

### Validation of experimental results

The experimental protocol and results are validated by comparing the forward and reconstructed signals obtained from the experiments for the ambient temperature condition with the FE simulation results. The forward responses received from the experiments and the FE analysis for a five-cycle tone burst excitation of 200 kHz central frequency normalized with respect to their respective peaks and are plotted in Figure 7(a) for comparison. The two results match well for both the symmetric  $S_0$  and antisymmetric  $A_0$  modes. Similar comparison for the normalized reconstructed signal after the TRP is presented in Figure 7(b) for both main and extended wave packets. The original input signal is also presented for verifying the quality of reconstruction of the Lamb wave response. The reconstructed signal obtained from the FE simulation is in excellent agreement with the original input waveform, validating the TRP simulation in the FE analysis. The reconstructed signal obtained from the experiment too

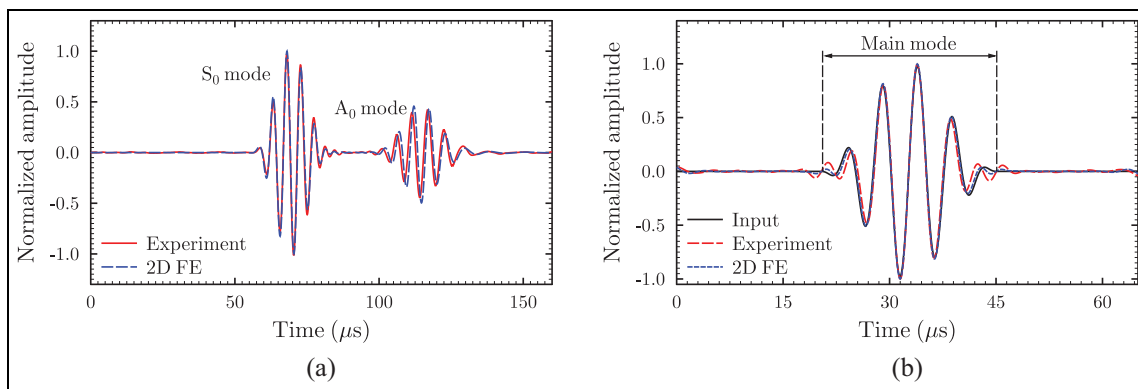


**Figure 7.** Comparison of experimental results with FE predictions for (a) forward response and (b) reconstructed signal (extended mode) under a five-cycle modulated tone burst excitation of 200 kHz frequency.



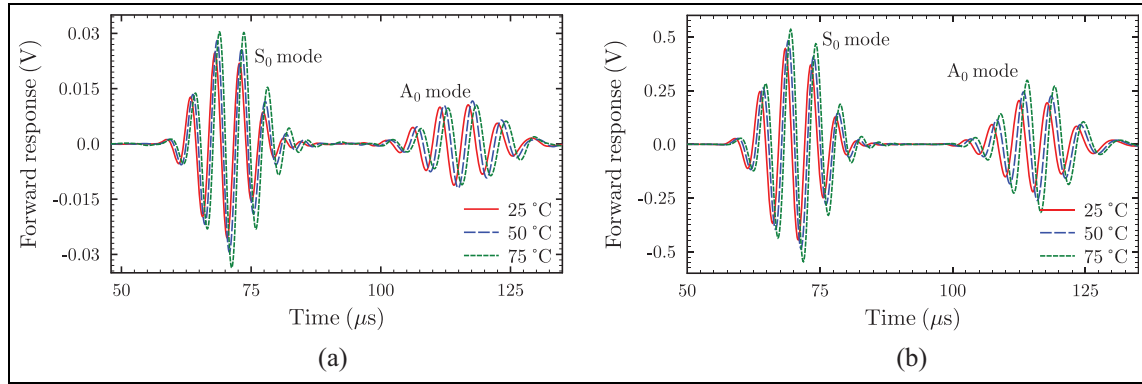


**Figure 8.** Effect of temperature on the forward Lamb wave response for a 200 kHz excitation in (a) experiment and (b) 2D FE simulation.

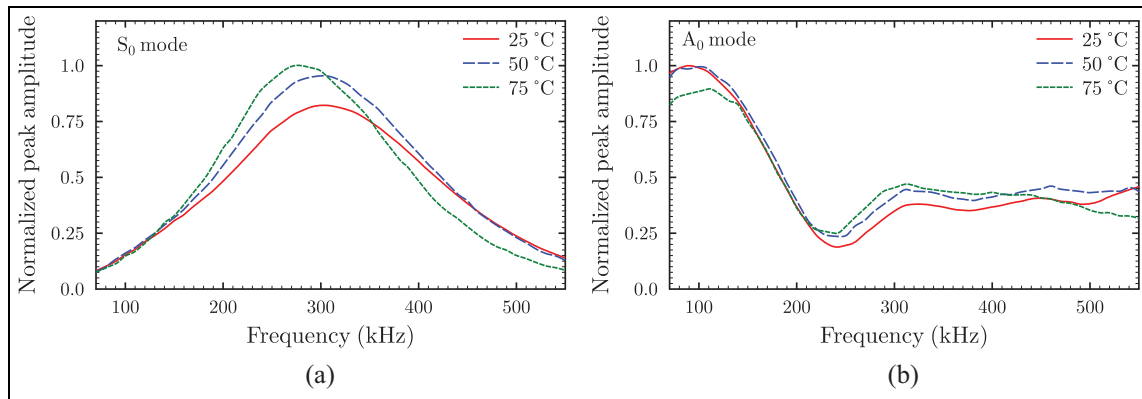


**Figure 9.** Normalized peak amplitude versus frequency curves obtained experimentally for different system temperatures for (a)  $S_0$  mode and (b)  $A_0$  mode.

matches well with the input signal except for a small deviation around the ends of the main mode. This deviation may be due to possible imperfect bonding between the transducers and the host plate in the experimental setup.

### Effect of temperature on forward response

Figure 8(a) shows the forward responses measured in the experiments for a 200 kHz excitation, with the plate temperature at 25°C, 50°C and 75°C. The corresponding results obtained from the FE simulations are plotted in Figure 8(b). Both the experimental and FE results display the same trend of an increase in the peak amplitude of the  $S_0$  mode with temperature rise in this case. The  $A_0$  mode too exhibits the same behaviour with temperature rise in the FE simulation. In the experiment, although the peak amplitude shows an increase with a temperature rise from 25°C to 50°C, it decreases when the temperature is raised to 75°C. This difference

between the experimental and FE simulation results can happen because of the possible unevenness of the adhesive layer thickness and other bonding imperfections in the experimental setup, which is not accounted for in the FE simulation. A delay in the time of arrival of the forward response is also observed with the rise in temperature in both results.

The amplitude change in the response signal occurs due to the increase in the piezoelectric coefficients, dielectric permittivities and elastic moduli of the piezoelectric transducers and decrease in the shear modulus of the araldite adhesive with an increase in temperature. The reduction in the adhesive shear modulus influences two opposite effects: (1) the shear lag effect which reduces the response amplitude and (2) the inertia effect which increases the same.<sup>35</sup> It explains why the amplitude of the  $A_0$  mode can increase or decrease with temperature depending on which of these two effects dominate. This has been elaborated further in the following discussions. The decrease in the elastic moduli

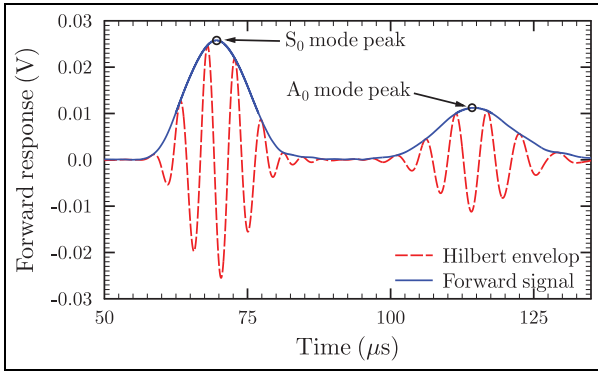


**Figure 10.** Hilbert envelope of the forward Lamb wave response under tone burst excitation of 200 kHz central frequency at 25°C. The peak amplitudes of the modes are obtained from this envelope.

of the aluminium plate with a temperature rise reduces the phase velocity of the  $S_0$  and  $A_0$  modes, resulting in the delay in the time of arrival of the forward response. The increase in the centre-to-centre distance between the transducers due to thermal expansion also contributes to this delay.

To examine if and how trends change with the excitation frequency, the variations of the peak amplitudes of the  $S_0$  and  $A_0$  modes obtained experimentally with the central excitation frequency are plotted in Figure 9 for the system temperatures of 25°C, 50°C and 75°C. The peak amplitudes of the different modes in the forward response are obtained from the Hilbert envelope. Figure 10 depicts the Hilbert envelope for the forward Lamb wave response under the tone burst excitation of 200 kHz central frequency at 25°C. To bring out the relative effect due to temperature rise, the plots in Figure 9 are normalized with respect to the maxima of all the three amplitude–frequency curves for the three

temperatures. The results presented in Figure 9 suggest that with the increase in the system temperature, the peak amplitude of the sensor signal may decrease or increase, depending on the excitation frequency and the Lamb wave mode. For the  $S_0$  mode, at the low and high frequencies over the probed frequency range of 70–550 kHz, the peak amplitude decreases with the increase in temperature (though the effect is small at low frequencies). This happens primarily due to the shear lag effect caused by the reduction in the adhesive shear modulus with the rise in temperature.<sup>25,35</sup> However, near the resonance frequency, the peak amplitude of the  $S_0$  mode increases with temperature, which can be attributed to the dominance of the dynamic effect over this frequency range. The resonance frequency itself shows a decrease with the increase in temperature. Ha et al.<sup>13</sup> have reported a similar trend of the amplitude variation with temperature.

For the  $A_0$  mode, the change in the peak amplitude with temperature shows a similar dependence on the excitation frequency, except that the decrease in the amplitude at low frequencies below 130 kHz is more significant unlike the case of  $S_0$  mode for temperature rise from 50°C to 75°C. A distinct increasing trend of the  $A_0$  mode amplitude with temperature is noticed for excitation frequencies beyond 220 and under 480 kHz. Again, this increase can be attributed to the predominance of the inertia effect over the shear lag effect for the  $A_0$  mode in this frequency range.

Many methods employ the time of arrival of Lamb waves for detecting and localizing damage. It has been observed earlier that the time of arrival increases with the increase in temperature. Figure 11 reveals that this delay in the time of arrival with temperature rise too is dependent on the excitation frequency. The change is small at low frequencies but becomes significant at higher frequencies. The effect is higher for the  $S_0$  mode than the  $A_0$  mode in the frequency range studied.

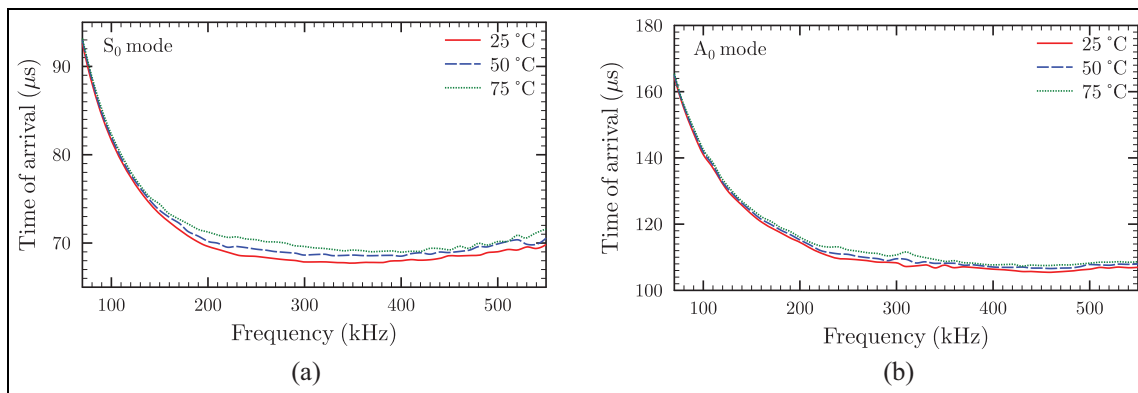


**Figure 11.** Time of arrival versus frequency curves obtained from experiments at different temperatures for (a)  $S_0$  mode and (b)  $A_0$  mode.

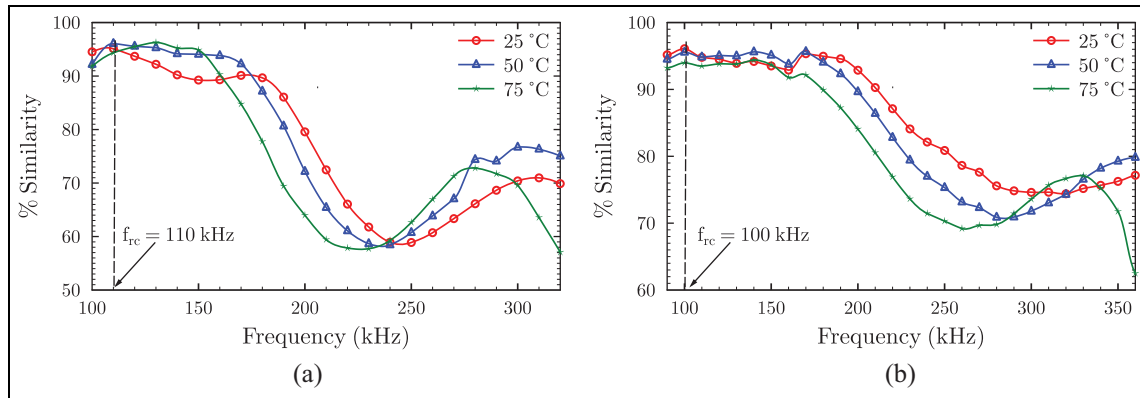


**Figure 12.** Effect of temperature on time reversibility of Lamb waves in a 3-mm aluminium plate, obtained from (a) experiment and (b) 2D FE simulation.

### Effect of temperature on time reversibility

While the temperature dependence of Lamb wave amplitude and time of arrival is expected and has been reported earlier, it is important to investigate if it leads to the temperature dependence of its time reversibility as well. To ascertain the effect of temperature on the time reversibility of Lamb wave, the percent similarity of the experimentally obtained reconstructed signal under the five-cycle tone burst excitation is plotted in Figure 12(a) as a function of the central excitation frequency for three values of system temperatures of 25°C, 50°C and 75°C. The percent similarity is calculated using the extended mode defined earlier. Figure 12(a) reveals that at room temperature, the best reconstruction occurs at a central excitation frequency of 110 kHz (best reconstruction frequency  $f_{rc}$ ) attaining the highest similarity of 95.1%. The percent similarity decreases to as low as 58.9% at an excitation frequency of 250 kHz. As explained earlier, the dependence of the reconstruction quality on the excitation frequency is due to the amplitude dispersion of Lamb waves. The results obtained for different temperature reveal that contrary to what is expected from a baseline-free method, the quality of reconstruction changes significantly with temperature variation in general. For an excitation frequency of 200 kHz, for instance, the percent similarity reduces significantly from 79.6% to 64.0% when the temperature is raised from 25°C to 75°C. However, at the best reconstruction frequency of 110 kHz, which was suggested to be the probing frequency in the RTRM proposed recently,<sup>25,36</sup> the similarity changes only marginally from 95.1% to 94.4% for the same temperature rise.

To verify this experimental observation, the same study is repeated using the FE simulation and the results are presented in Figure 12(b). The FE results

show very similar trends as the experiments. The best reconstruction frequency is obtained as 100 kHz at room temperature, which is fairly close to the experimentally obtained value of 110 kHz. The minor difference in the two values may be due to possible uneven thickness and imperfect bonding of the adhesive layers in the experimental setup. Furthermore, similar to the experimental results, in the simulation too, the percent similarity of the reconstructed signal is seen to undergo significant changes due to change in the system temperature, depending on the excitation frequency. At the excitation frequency of 230 kHz, for example, the similarity reduces from 84% to 73.6% when the temperature rises from 25°C to 75°C. At the best reconstruction frequency of 100 kHz, however, the percent similarity shows only a minor change from 96.1% to 94.0% for the same change in temperature, further validating the experimental outcomes. For a temperature up to 50°C, which is encountered in practice more commonly, the percent similarity at the best reconstruction frequency remains almost unchanged both in experiments and simulations. But, at other frequencies, it shows a significant change, for instance, by 9.7% at 210 kHz in the experiment and 7.0% at 260 kHz in the FE simulation.

The numerical study is further extended to a thinner aluminium plate of 1.5 mm thickness. Figure 13(a) plots the percent similarity of the reconstructed signal obtained from the FE analysis for the five-cycle tone burst excitation as a function of the excitation frequency for the system temperatures of 25°C, 50°C and 75°C. For this case too, there is a significant change in the percent similarity with temperature for all excitation frequencies over the studied range of 100–350 kHz except at the best reconstruction frequencies (137 kHz). To illustrate the effect of the tone burst count on time reversibility, the results for the same plate under an

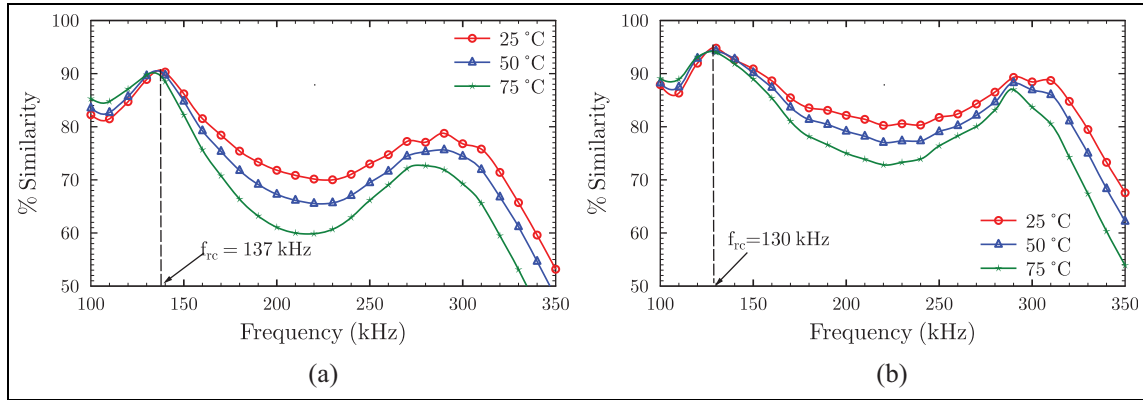


**Figure 13.** Effect of temperature on time reversibility of Lamb wave in a 1.5 mm plate, obtained from 2D FE simulation: (a) five-cycle tone burst excitation and (b) eight-cycle tone burst excitation.

eight-cycle tone burst excitation are shown in Figure 13(b) for the three temperatures. The higher tone burst count resulted in a higher percent similarity at all frequencies and temperatures in this case, while the best reconstruction frequency showed a marginal reduction to 130 kHz. Once again, the time reversibility is found to be significantly affected by temperature in general except at the best reconstruction frequency of 130 kHz.

It is thus established that the temperature invariance of time reversibility of Lamb waves, which is essential for the TRP to be used as a baseline-free method in the presence of environmental/operating temperature variability of the structure, holds well at the best reconstruction frequency and not at other probing frequencies in general.

### Role of individual constituents on temperature effects

In this section, we investigate, using the 2D FE model, how the individual constituents of the system contribute to the overall temperature dependence of the forward Lamb wave response and its time reversibility. The temperature of the plate, the adhesive layers and the piezoelectric transducers is varied one at a time from 25°C to 75°C keeping the other two unchanged at 25°C. The results are compared with the cases in which the whole system is maintained at the room temperature (25°C) and at the elevated temperature of 75°C. Figure 14 illustrates the variations of the peak amplitude of  $S_0$  mode of the forward response with the excitation frequency for the aforementioned five cases. A trend similar to that obtained in the experimental results (Figure 9) is observed in Figure 14 for the case when the system temperature as a whole is increased from 25°C to 75°C. For the system at 25°C, the resonance peak amplitude occurs at an excitation frequency of 350 kHz, whereas

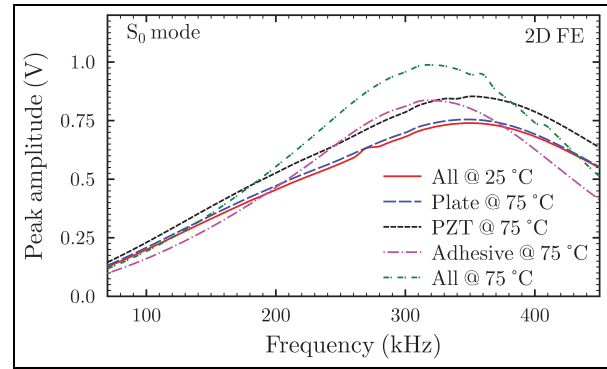


**Figure 14.** Frequency response of the  $S_0$  mode under the temperature of plate, transducers and adhesive layers individually and together to 75°C.

it shifts towards left to 320 kHz at the elevated temperature of 75°C. When only the plate's temperature is raised to 75°C, there is a minor increase in up to 2% in the amplitude of the forward response over the studied range of the excitation frequency and no change in the resonance frequency. The increase in the amplitude is due to the minor decrease in the elastic stiffness of the plate with temperature. Similarly, when only the piezoelectric transducers are heated to 75°C, the amplitude of the  $S_0$  mode increases without affecting the resonance frequency. In this case, however, the increase in the peak amplitude is substantial, being 16.1% at the resonance frequency. This change is primarily caused by the increase in the piezoelectric constants with temperature rise.

However, when only the adhesive layer is considered at the elevated temperature, the amplitude of the forward response actually shows a reduction for excitation

frequencies below 200 and above 380 kHz, while it shows an increase for the remaining middle frequency band around the resonance frequency. With an increase in its temperature, the shear modulus of the adhesive layers decreases, and the material damping increases. For frequencies away from the resonance frequency, the shear lag effect dominates and as a result, the decrease in the shear modulus of the adhesive layers with the rise in temperature leads to a decrease in the peak amplitude. The increase in material damping also adds to the reduction. Near the resonance frequency, however, the inertia effect becomes predominant over the shear lag effect and material damping effect, causing the rise in the peak amplitude. Furthermore, the resonance frequency shifts towards the left, which matches with the case of all the constituents being at 75°C. A maximum increase in 16.2% in the amplitude is observed at a frequency of 320 kHz, while a maximum decrease in 24.9% occurs at 450 kHz, for the frequency range considered. Thus, the overall trend in the amplitude change of Lamb wave due to temperature variation at different probing frequencies is primarily dictated by the change in the adhesive layer properties, whereas the temperature dependence of the adhesive layer shear modulus and damping, and the piezoelectric properties of the transducers constitute the most influencing parameters for the change in the response amplitude at a given frequency.

A similar study is conducted next on the role of the individual constituents on the temperature dependence of time reversibility of Lamb waves. The percent similarities for all the five cases are compared in Figure 15 for excitation frequencies ranging from 90 to 360 kHz. When the temperature of the plate or the PZT layer is elevated to 75°C individually, the percent similarity does not show any appreciable change from the case when the whole system is at 25°C for the entire frequency range. However, when only adhesive layer temperature is increased, the percent similarity changes significantly, matching closely with the percent similarity obtained when all the constituents are at 75°C. It is thus evident that the adhesive layer is primarily responsible for the change of time reversibility of Lamb waves in plates actuated and sensed by surface-bonded piezoelectric transducers, due to the change in the environmental/operating temperature.

## Conclusion

A detailed study has been performed on the effect of the temperature variation on the forward response and the time reversibility of Lamb waves propagating in a

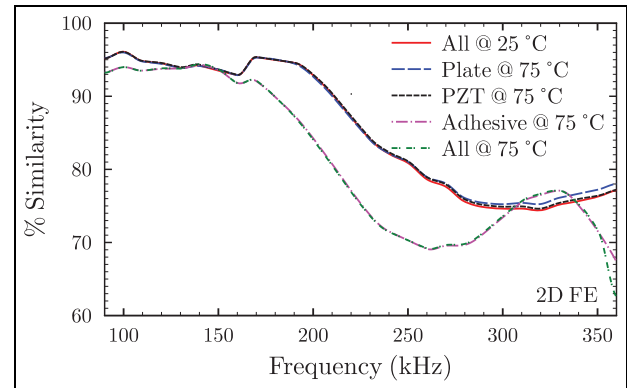


**Figure 15.** Time reversibility-frequency variations for the temperature rise of plate, transducers and adhesive layers individually and together to 75°C.

thin plate, actuated and sensed by surface-bonded piezoelectric wafer type transducers, using experiments and 2D FE simulations. The investigation has been conducted for three values of the temperatures 25°C, 50°C and 75°C, each for a wide range of the excitation frequency. The study has revealed the following:

1. The sensor signals of Lamb wave response measured after repeated thermal cycles revealed that the response remains unchanged after the first cycle. This result signifies that the araldite adhesive provides a stable performance and thus makes a good choice for bonding transducers for SHM applications under varying thermal environments.
2. The 2D FE results for the normalized forward response and the reconstructed signal match well with the experimental results and are able to capture all the significant trends observed in the experiments.
3. The amplitude of the forward response may increase or decrease with the temperature rise depending on the excitation frequency. The amplitude increases with temperature over a frequency band around the resonance frequency due to the dominant transducer inertia effect. At lower and higher frequencies away from the resonance frequency, the amplitude shows a decrease with temperature due to the shear lag and damping effects.
4. The amplitude change in the response signal with temperature variation is mostly contributed by the change in the piezoelectric properties of the transducers, and shear modulus and damping of the adhesive layer. However, the overall trend of increase and decrease in the amplitude with

temperature at different excitation frequency is primarily influenced by the change in material properties of the adhesive layers.

5. The change in the time of arrival of Lamb waveforms due to the temperature rise depends on the excitation frequency and is significant for higher frequencies.
6. The experimental and FE simulation studies revealed that the temperature invariance of the time reversibility, which is essential for the Lamb wave TRM to be used as a baseline-free method for damage detection under variable temperature conditions, does not hold good in general. At the best reconstruction frequency (a concept proposed by Agrahari and Kapuria),<sup>22,23</sup> however, the variation of the percent similarity of the reconstructed signal with temperature is insignificant.
7. The numerical study reveals that the variation of the material properties of the plate and the piezoelectric transducers with temperature has a negligible effect on the quality of reconstruction of the TRP. The temperature dependence of the time reversibility of the Lamb wave is almost wholly contributed by the change in the material properties of the adhesive layers.

This study thus reveals that it may not be generally possible to use the conventional TRM as a baseline-free method of damage detection under variable temperature conditions, due to the temperature dependence of the time reversibility of Lamb waves. However, the RTRM (which proposes to probe the structure at the best reconstruction frequency)<sup>22,23,36</sup> can be potentially used as a baseline-free method even in the presence of environmental/operating temperature variations, as the time reversibility of Lamb waves is nearly temperature invariant at this frequency.

#### Declaration of conflicting interests


The author(s) declared no potential conflicts of interest with respect to the research, authorship and/or publication of this article.

#### Funding

The author(s) disclosed receipt of the following financial support for the research, authorship and/or publication of this article: S. Kapuria acknowledges the financial support for this work provided by the Science and Engineering Research Board, Department of Science and Technology, Government of India through J. C. Bose National Fellowship (Grant No. JCB/2018/000025).

#### ORCID iDs

Bhabagrahi Natha Sharma  <https://orcid.org/0000-0001-7512-4962>

Santosh Kapuria  <https://orcid.org/0000-0003-1172-1279>

#### References

1. Su Z and Ye L. *Identification of damage using Lamb waves*. Berlin: Springer, 2009.
2. Sohn H. Effects of environmental and operational variability on structural health monitoring. *Philos Trans Royal Soc Struct Health Monit* 2007; 365: 539–560.
3. Blaise E and Chang F. Built-in diagnostics for debonding in sandwich structures under extreme temperatures. In: *Proceedings of the 3rd international workshop on structural health monitoring*, Stanford, California, USA, 12–14 September 2001, pp. 154–163. Florida, USA: CRC Press.
4. Lee B, Manson G and Staszewski W. Environmental effects on Lamb wave responses from piezoceramic sensors. *Mater Sci Forum* 2003; 440: 195–202.
5. Chambers J, Wardle B and Kessler S. Durability assessment of Lamb wave-based structural health monitoring nodes. In: *Proceedings of the 47th AIAA/ASME/ASCE/AHS/ASC structures, structural dynamics, and materials conference*, Newport, RI, 1–4 May 2006, p. 2263. Reston, VA: AIAA.
6. Schulz MJ, Sundaresan MJ, McMichael J, et al. Piezoelectric materials at elevated temperature. *J Intel Mater Syst Struct* 2003; 14(11): 693–705.
7. Konstantinidis G, Drinkwater B and Wilcox P. The temperature stability of guided wave structural health monitoring systems. *Smart Mater Struct* 2006; 15(4): 967.
8. Lu Y and Michaels JE. A methodology for structural health monitoring with diffuse ultrasonic waves in the presence of temperature variations. *Ultrasonics* 2005; 43(9): 717–731.
9. Raghavan A and Cesnik CE. Studies on effects of elevated temperature for guided-wave structural health monitoring. In: *Proceedings of the 14th SPIE international symposium on smart structures and materials/NDE and health monitoring*, San Diego, CA, 18–22 March 2007, cp65290A. Bellingham, WA: SPIE.
10. Scalea FLD and Salamone S. Temperature effects in ultrasonic Lamb wave structural health monitoring systems. *J Acoust Soc Am* 2008; 124(1): 161–174.
11. Andrews JP, Palazotto AN, DeSimio MP, et al. Lamb wave propagation in varying isothermal environments. *Struct Health Monit* 2008; 7(3): 265–270.
12. Han SJ, Palazotto AN, ASCE F, et al. Finite-element analysis of Lamb wave propagation in a thin aluminium plate. *J Aerospace Eng* 2009; 22: 185–197.
13. Ha S, Lonkar K, Mittal A, et al. Adhesive layer effects on PZT-induced Lamb waves at elevated temperatures. *Struct Health Monit* 2010; 9(3): 247–257.
14. Kijanka P, Packo P, Zhu X, et al. Three-dimensional temperature effect modelling of piezoceramic transducers

- used for Lamb wave based damage detection. *Smart Mater Struct* 2015; 24(6): 065005.
15. Croxford AJ, Wilcox PD, Konstantinidis G, et al. Strategies for overcoming the effect of temperature on guided wave structural health monitoring. In: *Health monitoring of structural and biological systems International Society for Optics and Photonics*, San Diego, CA, 11 April 2007, p. 65321T. Bellingham, WA: SPIE.
  16. Dao PB and Staszewski WJ. Cointegration approach for temperature effect compensation in Lamb-wave-based damage detection. *Smart Mater Struct* 2013; 22(9): 095002.
  17. Fink M. Time-reversal of ultrasonic fields-Part I: basic principles. *IEEE T Ultrason Ferroelectr Frequen Control* 1992; 39(5): 555–566.
  18. Xu B and Giurgiutiu V. Single mode tuning effects on Lamb wave time-reversal with piezoelectric wafer active sensors for structural health monitoring. *J Nondestruct Eval* 2007; 26: 123–134.
  19. Santoni GB, Yu L, Xu B, et al. Lamb wave-mode tuning of piezoelectric wafer active sensors for structural health monitoring. *J Vib Acoust T ASME* 2007; 129(6): 752–762.
  20. Gangadharan R, Murthy CRL, Gopalakrishnan S, et al. Time-reversal technique for health monitoring of metallic structure using Lamb waves. *Ultrasonics* 2009; 49: 696–705.
  21. Miao X, Wang D, Ye L, et al. Identification of dual notches based on time-reversal Lamb waves and a damage diagnostic imaging. *J Intel Mater Syst Struct* 2011; 22: 1983–1992.
  22. Agrahari JK and Kapuria S. A refined Lamb wave time-reversal method with enhanced sensitivity for damage detection in isotropic plates. *J Intel Mater Syst Struct* 2016; 27(10): 1283–1305.
  23. Agrahari JK and Kapuria S. Active detection of block mass and notch-type damages in metallic plates using a refined time-reversed Lamb wave technique. *Struct Control Health Monit* 2017; 25(2): e2064.
  24. Lee SJ, Sohn H and Hong JW. Time reversal based piezoelectric transducer self-diagnosis under varying temperature. *J Nondestruct Eval* 2010; 29(2): 75–91.
  25. Agrahari JK and Kapuria S. Effect of adhesive, host plate, transducer and excitation parameters on time reversibility of ultrasonic Lamb waves. *Ultrasonics* 2016; 70: 147–157.
  26. Sharma BN, Kapuria S and Arockiarajan A. Effect of temperature on time reversibility of Lamb wave in thin plates with surface-bonded piezoelectric wafers. *Struct Health Monit* 2019; 2019: 1945–1952.
  27. Moser F, Jacobs LJ and Qu J. Modeling elastic wave propagation in wave guides with the finite element method. *Non Destruct Test Eval Int* 1999; 32: 225–234.
  28. Epoxy. Araldite epoxy, 2008, <https://www.kremer-pigment.com/media/pdf/97930.pdf> (accessed 26 April 2019).
  29. Sparkler. Sparkler piezoceramics, 2018, <http://www.sparklceramics.com/piezoelectricproperties.html> (accessed 23 February 2018).
  30. Sherrit S, Yang G, Wiederick H, et al. Temperature dependence of the dielectric, elastic and piezoelectric material constants of lead zirconate titanate ceramics. In: *Proceedings of the international conference on smart materials, structures and systems*, Bangalore, India, 7–10 July 1999, pp. 7–10. New Delhi: Allied Publishers.
  31. Hooker MW. Properties of PZT-based piezoelectric ceramics between-150 and 250 c, 1998, <https://ntrs.nasa.gov/citations/19980236888>
  32. Beards C. *Structural vibration: analysis and damping*. New York: Elsevier, 1996.
  33. Bhalla S and Soh CK. Structural health monitoring by piezo-impedance transducers. I: modeling. *J Aerosp Eng* 2004; 17(4): 154–165.
  34. Nader G, Silva EN and Adamowski JC. Effective damping value of piezoelectric transducer determined by experimental techniques and numerical analysis. In: *ABCM symposium series in mechatronics*, 2004, pp. 271–279, [http://www.abcm.org.br/symposium-series/SSM\\_Vol1/Section\\_II\\_Control\\_Systems/SSM\\_II\\_14.pdf](http://www.abcm.org.br/symposium-series/SSM_Vol1/Section_II_Control_Systems/SSM_II_14.pdf)
  35. Kapuria S, Sharma BN and Arockiarajan A. Dynamic shear-lag model for stress transfer in piezoelectric transducer bonded to plate. *AIAA J* 2018; 57(5): 2123–2133.
  36. Kannusamy M, Kapuria S and Sasmal S. Accurate baseline-free damage localization in plates using refined Lamb wave time-reversal method. *Smart Mater Struct* 2020; 20: 05504417.